Available online at www.sciencedirect.com
ScienceDirect
Earth and Planetary Science Letters 260 (2007) 394–406
EPSL
www.elsevier.com/locate/epsl

A 48-kyr-long slip rate history for the Jordan Valley segment of the Dead Sea Fault

Matthieu Ferry [a,*], Mustapha Meghraoui [a], Najib Abou Karaki [b], Masdouq Al-Taj [c], Hani Amoush [b], Salman Al-Dhaisat [d], Majdi Barjous [e]

[a] Institut de Physique du Globe, UMR 7516, 5 rue René Descartes, 67084 Strasbourg, France
[b] Department of Environmental and Applied Geology, University of Jordan, Amman 11942, Jordan
[c] Department of Earth and Environmental Sciences, The Hachemite University, P.O. Box 150459, Zarqa 13115, Jordan
[d] Al-Balqa Applied University, Royal Jordanian Geographic Centre College for Survey Sciences, P.O. Box 414, Al-Jubaiha 11941, Jordan
[e] Natural Resources Authority, P.O. Box 7, Amman 11118, Jordan

Received 23 November 2006; received in revised form 4 May 2007; accepted 10 May 2007
Available online 12 June 2007
Editor: T. Spohn

Abstract

We investigate the late Quaternary active deformation along the Jordan Valley segment of the left-lateral Dead Sea Fault and provide new insights on the behaviour of major continental faults. The 110-km-long fault segment shows systematic offsets of drainage systems surveyed at three sites along its southern section. The isotopic dating of six paleoclimatic events yields a precise chronology for the onset of six generations of gully incisions at 47.5 ka BP, 37.5 ka BP, 13 ka BP, 9 ka BP, 7 ka BP, and 5 ka BP. Additionally, detailed mapping and reconstructions provide cumulative displacements for 20 dated incisions along the fault trace. The individual amounts of cumulative slip consistently fall into six distinct classes. This yields: i) an average constant slip rate of 4.7 to 5.1 mm/yr for the last 47.5 kyr and ii) a variable slip rate ranging from 3.5 mm/yr to 11 mm/yr over 2-kyr- to 24-kyr-long intervals. Taking into account that the last large earthquake occurred in AD 1033, we infer 3.5 to 5 m of present-day slip deficit which corresponds to a Mw ~7.4 earthquake along the Jordan Valley fault segment. The timing of cumulative offsets reveals slip rate variations critical to our understanding of the slip deficit and seismic cycle along major continental faults.

Keywords: Dead Sea fault; active tectonics; geomorphology; paleoclimatology; fault slip rate

1. Introduction

The active deformation associated with large continental faults often displays prominent tectonic landforms mainly due to the occurrence of successive large earthquakes in the past. The north–south trending left-lateral Dead Sea transform fault (DSF), a ~1000-km-long major plate boundary accommodates most of the active deformation between the Arabian and African–Sinai plates (Fig. 1). Taking the historical seismicity of the region into account (Abou Karaki, 1987; Ambraseys and Jackson, 1998; Sbeinati et al., 2005), the fault was likely the source of several large earthquakes ($M>7$) with severe damage, surface faulting and landscape changes. A segment of the DSF zone that shows pull-apart basins and transpressive ridges along strike is well exposed in the Jordan Valley where it extends from the Dead Sea to the

* Corresponding author.
E-mail address: matthieu.ferry@eost.u-strasbg.fr (M. Ferry).

0012-821X/$ - see front matter © 2007 Elsevier B.V. All rights reserved.
doi:10.1016/j.epsl.2007.05.049

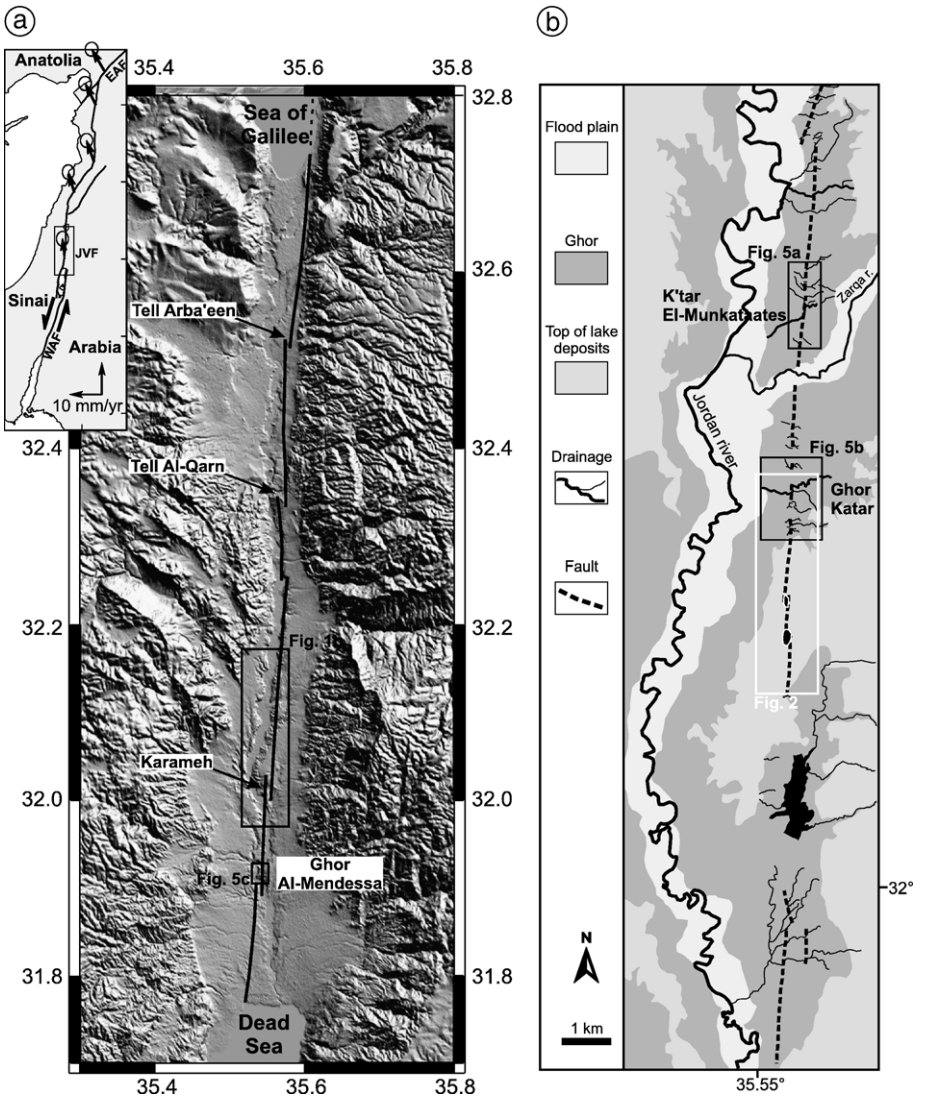

Fig. 1. a) Location of the Dead Sea fault (black line) in the Jordan Valley between the Sea of Galilee and the Dead Sea. The fault rupture appears to be sub-divided into fault sub-segments by prominent pressure ridges at Tell Arba'een, Tell Al-Qarn and Karameh. Inset shows plate tectonics in the eastern Mediterranean with GPS velocities (McClusky et al., 2003). Shaded topography is from 90-m-resolution SRTM3f data. b) Geomorphological map of the Jordan Valley around Karameh. Most prominent units include the badland-type Ghor areas, which contain a dense network of deeply incised streams and that separate the flat top surface of Lisan and Damya units and the flood plain of the present-day Jordan River. The Ghor area exhibits numerous natural outcrops and provides favourable fault mapping conditions.

Sea of Galilee (Fig. 1a). The fault segmentation, successive co-seismic displacements, and timing of past large earthquakes are, however, not well established along the fault zone and require field investigations in earthquake geology.

The Jordan Valley exposes a continuous stratigraphic section of lacustrine deposits (Lisan and Damya formations; Landmann et al., 2002) that spans the last 65 kyr. This remarkable sedimentary formation, with successive paleoshores and high-resolution isotopic analysis of aragonite- and gypsum-rich units represent a unique record for paleoclimatology (Enzel et al., 2006). The late Pleistocene and Holocene lacustrine deposits and related drainage network that cover the major part of the rift valley, likely constitute a geological archive of the successive fault movements.

Previous estimates of slip rates along the DSF vary from 2 to 10 mm/yr (Garfunkel et al., 1981; Galli, 1999; Niemi et al., 2001). According to historical documents, the most recent large earthquakes along the Jordan Valley fault (JVF) occurred in 749 AD and 1033 AD and severely damaged ancient cities of the Jordan Valley (Guidoboni

et al., 1994). Earthquakes are also reported at the archaeological sites of Pella, Jerash, and Tell El-'Umayri (near Amman) (Savage et al., 2003; Marco et al., 2003) and testify to the long-term seismic activity in the Jordan Valley area. These historical and pre-historical earthquakes may have produced surface faulting with significant cumulative left-lateral offsets.

In this paper, we document surface ruptures and describe evidence of systematic cumulative offsets affecting drainage networks at three sites along the southern section of the JVF. The well-dated Lisan and Damya late Quaternary lacustrine formations and related high resolution climatic fluctuations allow the long term slip rate along the fault to be constrained.

Finally, the slip rate along the DSF, its relationship with fault behaviour, and implications of this slip rate for the earthquake hazard assessment are discussed.

2. Late Quaternary stratigraphy of the Jordan Valley

The available high-resolution stratigraphic sequence is a key factor for the understanding of geological phenomena in the valley. Pleistocene formations display varved lacustrine sediments of Lake Lisan, a precursor of the Dead Sea. Locally, the retreat of Lake Lisan was followed by the late Pleistocene onset of the freshwater Lake Damya (Abed and Yaghan, 2000). The Lisan and Damya formations have been the subject of extensive geological and geochemical studies that provide extremely detailed stratigraphic descriptions along with U–Th and ^{14}C ages ranging from 63 ka BP to 12 ka BP (Bartov et al., 2002; Landmann et al., 2002; Haase-Schramm et al., 2004). Northeast of the Dead Sea in the Ghor Katar area (Figs. 1b, 2 and 3), Abed and Yaghan (2000) and Haase-Schramm et al. (2004) describe in detail the stratigraphic log and paleoclimatic correlations using varve-counting and isotopic dating in outcrops from deep (>40 m) river incisions. The stratigraphy is made of: i) a lower unit with laminated calcareous silt, aragonite and well-individualized sand and gravel layers (54–67.5 ka BP), ii) a middle unit made of massive clays (27–54 ka BP) and iii) an upper unit of intercalated laminated silt and aragonite (15–27 ka BP). In places, the uppermost Lisan units are overlain by a noticeable freshwater sandy deposit that corresponds to the Holocene Damya formation.

Lacustrine units consist in horizontal laminae visible across large areas in wide incisions where local variations are due to landslides, seismites and backtilting against normal faults.

3. Erosional landforms and paleoclimatic fluctuations

Geomorphologic markers such as incisions in lacustrine deposits and paleoshorelines result from landform processes that are partly controlled by climatic fluctuations. A straightforward observation in the Jordan Valley is that the uppermost shoreline level is at −190 m, while the present-day level of the Dead Sea is at −417 m, showing a lake-level drop of 227 m in the last 25 kyr (Fig. 2) and attesting to an increasingly arid climate. Moreover, we observe that the present-day flat topography (top of the lacustrine units) of the valley has an elevation ranging from −295 m to −320 m in the southern section of the valley. Lacustrine units are affected by well-developed gully networks corresponding to secondary tributaries of the Jordan River (ghor in Fig. 1b). The erosional process responsible for the drainage network (gullies) is mainly controlled by the

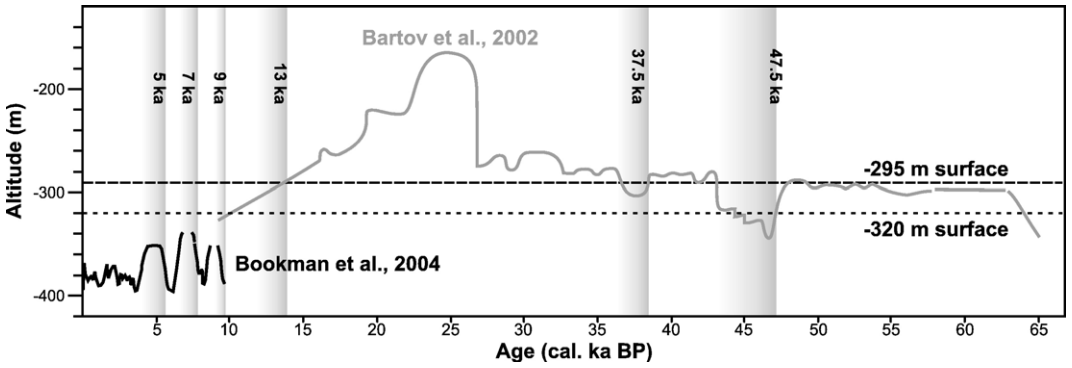

Fig. 2. Level fluctuations of Lake Lisan (grey curve) and rainfall history of the subsequent Dead Sea (black curve) compiled from Bartov et al. (2002) and Bookman et al. (2004). Dashed lines indicate the elevation of the surface topography at K'tar El-Munkataates and Ghor Katar (long dashes, −295 m) and Ghor Al-Mendessa (short dashes, −320 m). Shades of grey point to the interpreted onsets of the six generations of gully incisions (the darker the most likely).

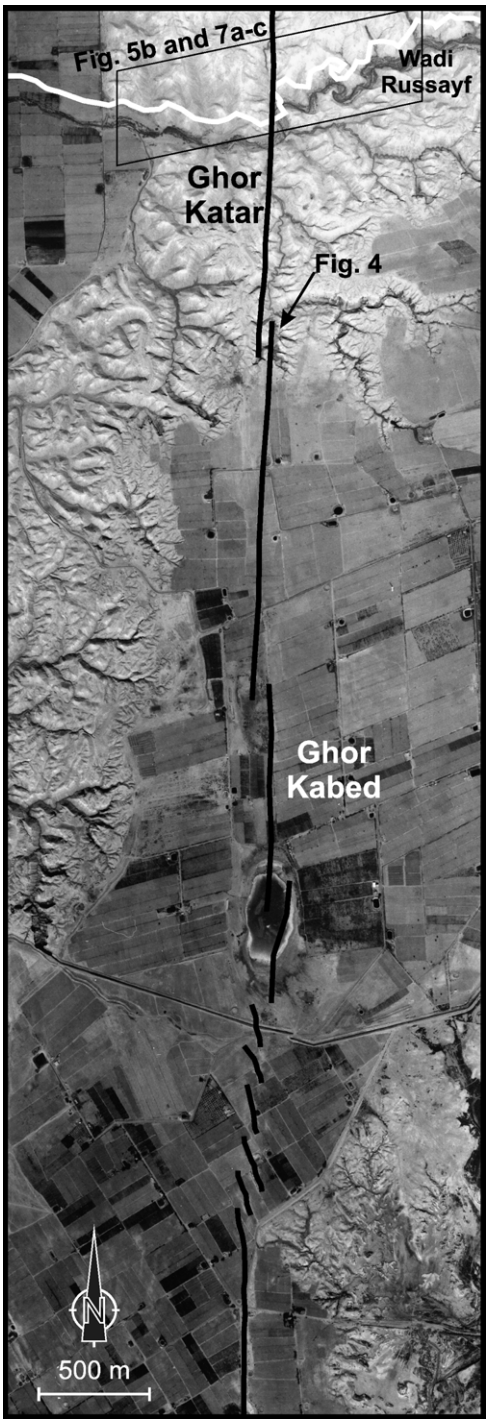

Fig. 3. Aerial photograph (original scale of 1:20,000) of the area between Ghor Kabed and Wadi Russayf. The conspicuous fault trace displays en-echelon features, pull-apart basins and left- laterally offset drainage systems. See Fig. 1b for location.

down-drop of the lake water level and reflects paleoclimatic fluctuations. Therefore, the combined analysis of visible geomorphologic processes and detailed description and dating of late Pleistocene – Holocene sedimentary units allow for a high-resolution paleoclimatic reconstruction.

Bartov et al. (2002) studied lake-level fluctuations from radiocarbon-dated subaerial to deep lacustrine and fan delta sedimentary sequences and terraces west of the Dead Sea and provide with a well-constrained lake-level curve during the late Pleistocene. On the basis of radiocarbon-dated paleoshores, post-Damya rainfall history was recently improved by Bookman et al. (2004). The authors provide a high-resolution record of lake-level fluctuations during the Holocene showing strong gradients involving rise or fall episodes of ~50 m in ~500 yr-periods (i.e. at a rate of 10 cm/yr) and correlate those level fluctuations with intense rainfall episodes triggered by large-scale atmospheric circulation. A compilation of lake-level curves (Fig. 2) yields a continuous record of rainfall periods and the related lake-level variations during the last 65 ka. Since the Lisan chronology is well established and lake-level drops occur at a fast rate, the occurrence of paleoclimatic events may be determined with a conservative uncertainty of 500 yr. For the Holocene, more accurate records allow for a reduced uncertainty of 100 yr.

The onset and development of gully incisions affecting Lisan and Damya units is crucial for the understanding of successive fault movements. The Dead Sea fault intersects numerous ghor areas (drainage networks) that provide clear natural exposures in the Jordan Valley (between 31°47′ N and 32°30′ N latitudes). Gullies are generally initiated during strong precipitation events on soft sedimentary units and are likely to remain, especially under arid climates (Bloom, 1991). Two processes may explain the formation of gullies incising the top of lacustrine deposits: i) if the lake level falls below the elevation of the surface, newly exposed water-saturated soft sediments are very likely to be strongly eroded and gullies start forming immediately. ii) if the lake level is already lower than the ground surface, intense rainfall events are also likely to prompt the inception of new gullies (Poesen et al., 2003) ready to record subsequent fault movements.

In summary, a total of six climatic events likely to have triggered the onset of incisions from the maximum surface elevation at −295 m have been identified for the last 65 ka, i.e. since the early deposition of Lisan units. Fig. 2 (Bartov et al., 2002; Bookman et al., 2004) illustrates three lake-level drops below that elevation at 47.5±0.5 ka BP, 37.5±0.5 ka BP and 13±0.5 ka BP and three intense rainfall episodes at 9±0.1 ka BP, 7±0.1 ka BP and 5±0.1 ka BP. This implies the likely onset of six generations of incisions during that timeframe.

4. The Jordan Valley fault segment

The Jordan Valley is a major tectonic depression formed as a rift that accumulated ~5 km of Quaternary sediments (Garfunkel et al., 1981). Examination of satellite (SPOT 5 at 5 m resolution and Landsat 7 at 14.5 m resolution) and aerial photos (1:20,000 scale) combined with field investigations allowed us to map a major part of the fault segment. Large pull-apart basins (>10 km) of the Sea of Galilee and Dead Sea constitute the boundaries of the ~110-km-long fault segment (Fig. 1a). The segment is made of linear strands that show left-lateral offsets of drainage systems, right-stepping ruptures with pressure and shutter ridges, and small pull-apart basins along strike (Al-Taj, 2000 and Figs. 1 and 3 herein). At the outcrop level, observed buried major and minor faults and seismites are similar to those described by Reches and Hoexter (1981), El-Isa and Mustafa (1986), Marco et al. (1996), Malkawi and Alawneh (2000) and Marco et al. (2005) in the Lisan and Damya (Figs. 1b and 4).

In numerous sections along the fault, a young scarp delineates the surface deformation and attests to late Pleistocene and Holocene tectonic movements with cumulative displacements. Two major pull-apart basins (namely the Sea of Galilee and the Dead Sea) structurally control the extent of the JVF segment. The inner part of the segment may be sub-divided in several fault sub-segments limited by right-stepping fault structures mainly. Field observations combined with aerial photos indicate the existence of three main pressure ridges, from north to south at Tell Arba'een, Tell Al-Qarn and Karameh (Fig. 1a). These pressure ridges indicate a complex structural pattern of at least four 16- to 45-km-long fault sub-segments. Furthermore, the only visible extensional relay zones along strike are the two few-hundred-meters-long pull-apart basins located at Ghor Kabed, north of Karameh (Figs. 1b and 3). Additionally, the gullies expose impressive fault sections showing vertical offsets in late Quaternary units (Fig. 4). The measured vertical offsets at Ghor Katar (Fig. 1b) are 10.7± 0.2 m for the "white cliff", 13.5±0.3 m for the base of the upper Lisan and 18.4±0.5 m for the middle Lisan (Fig. 4). One may also observe that the fault subdivides into branches localized in a narrow zone (<500 m wide) and affects young sedimentary units up to the surface.

Although the JVF segment appears to be made of four fault sub-segments, the large- scale geometry of the

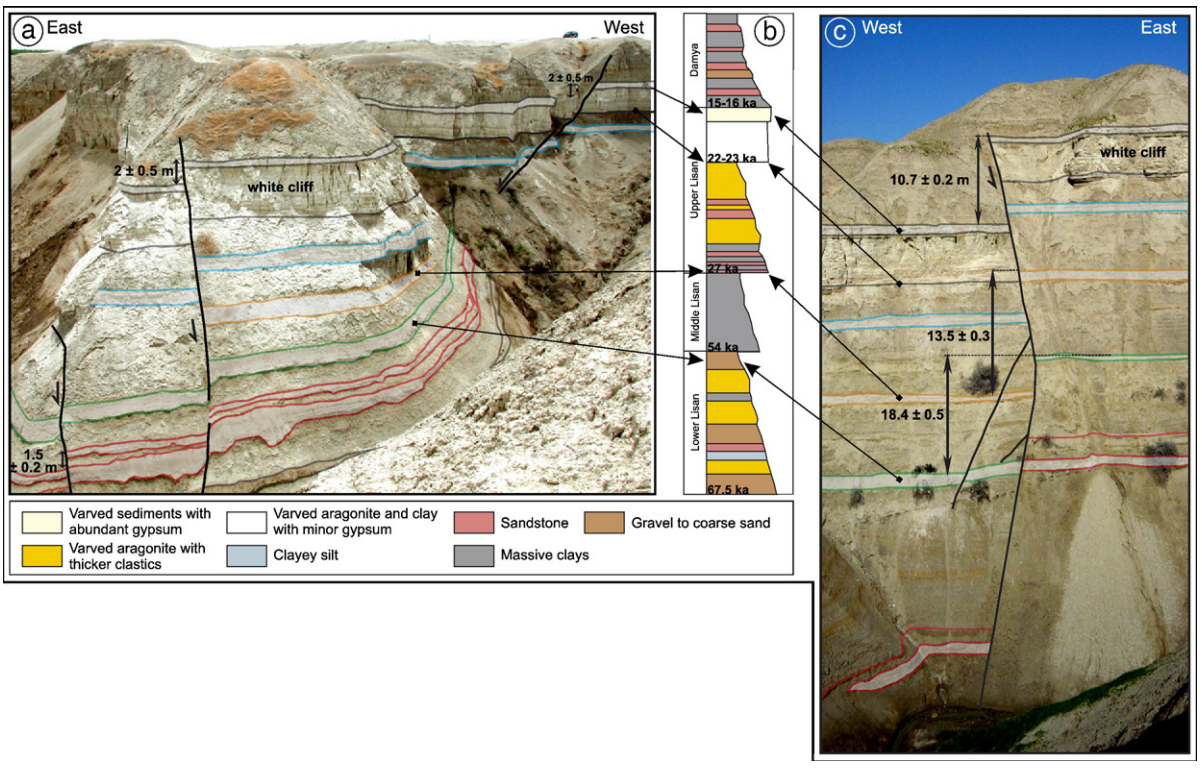

Fig. 4. JVF exposures at Ghor Katar (see Figs. 1b and 2 for location). Deep incisions reveal the Damya and Lisan units that are affected by three major fault branches showing a total of 18.4±0.5 m of vertical displacement. The topmost units are located at an elevation of ~−295 m.

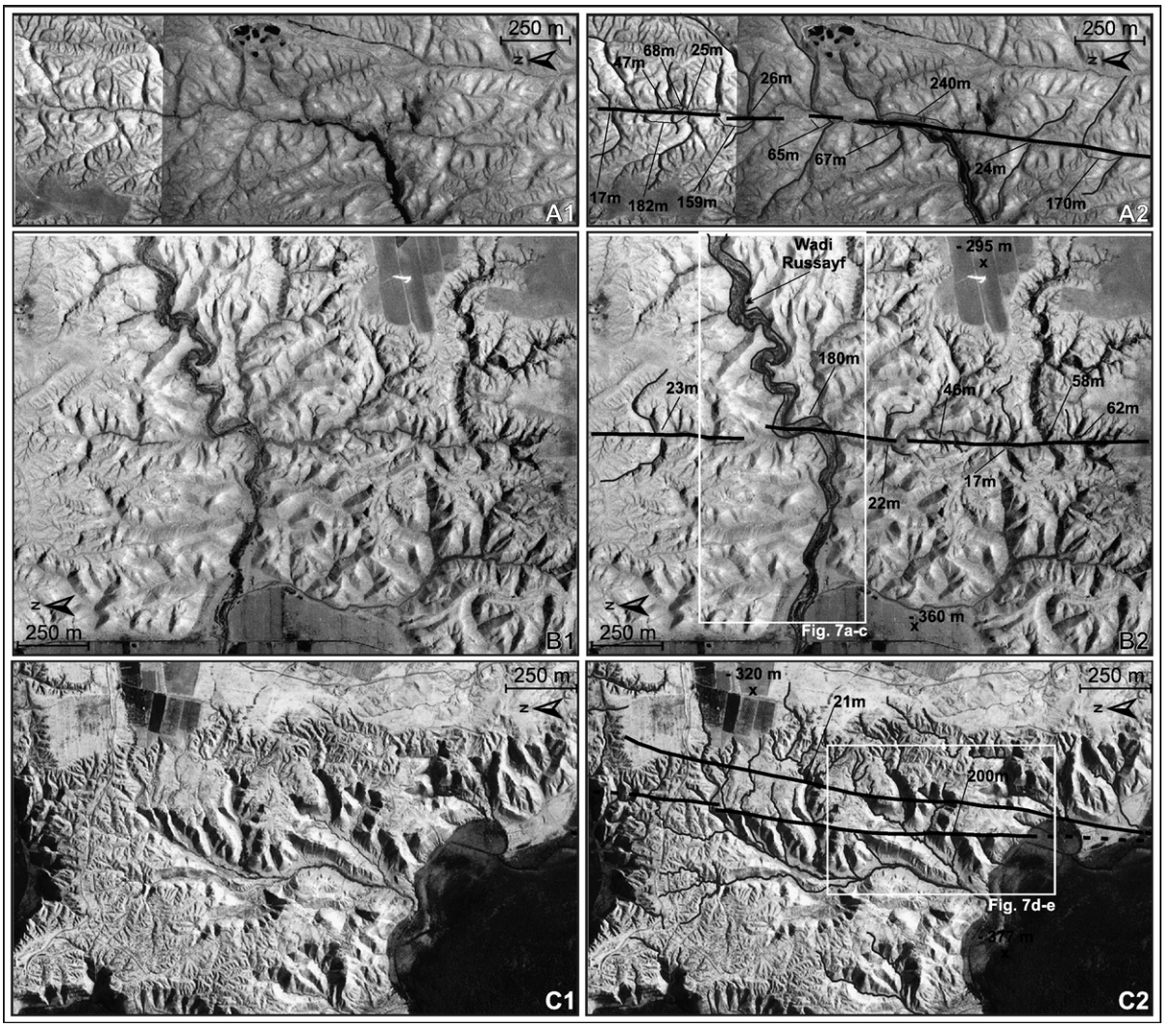

Fig. 5. A1, B1 and C1) Aerial photographs showing offset gullies and streams used in the present study (see Fig. 1 for location). A2, B2 and C2) Interpreted photographs. Thick black lines are active faults, thin lines are drainage, numbers refer to the measured cumulative left-lateral displacements. A1 and A2) K'tar El-Munkataates area (32°07′ N, 35°34′ E). This region shows a set of nine offset incisions with a notably deeper and older stream affected by a total offset of 240±20 m. B1 and B2) Ghor Katar area (32° 05′ N, 35° 33′ E). This site displays a clear example with the Wadi Russayf for which a reconstruction yields a total offset of 180±20 m (see reconstruction in Fig. 7a–c). C1 and C2) Ghor Al-Mendessa area (31°55′ N, 35°32′ E). This region is located inside a large meander loop of the Jordan River and is affected by two main fault branches as well as several minor splays not shown here. The deepest incisions are displaced by 200 m by the main fault and 21 m by a secondary fault (see reconstruction in Fig. 7e).

110-km-long rupture is typical of a seismic source for a Mw 7–7.5 earthquake (Wells and Coppersmith, 1994). Beside the large-scale pull-apart basins (Dead Sea and Sea of Galilee) that form the segment boundaries, the relatively small size of transtensional and transpressional stepovers (<2 km) may not constitute an important structural obstacle to the propagation of earthquake ruptures (Wesnousky, 2006).

Historical earthquakes in the area are well documented in the medieval times and the location of maximum damage zones is accurately known. Marco et al. (2003) document the AD 749 earthquake and report the distribution of intensity X MMS (Mercalli Modified Scale) at several locations between the Sea of Galilee and the Dead Sea. The valley experienced another earthquake in AD 1033 that damaged the same area between Jericho and the Sea of Galilee (Poirier and Taher, 1980; Abou Karaki, 1987) suggesting it had the same seismic source as the AD 749 earthquake. The location of the two events within the Jordan Valley and the related

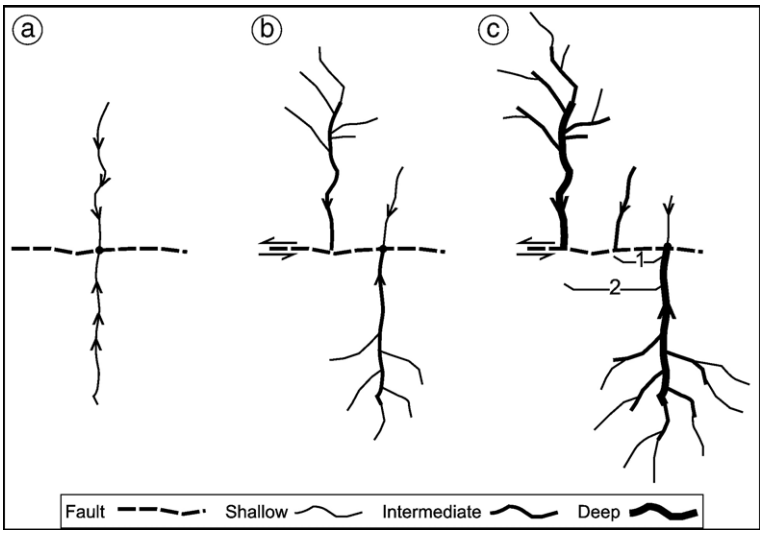

Fig. 6. Recording of cumulative offsets by a regressive erosion network. a) The fault produces a weak line along which gully inception may initiate (black dot). b) The pre-existing drainage network extends in terms of size and depth while being offset by the fault. Original inception points may trigger the development of new gullies. c) Further development produces a situation visible in Fig. 5A and B and shows the importance of depth analysis to match corresponding gullies across the fault. 1 and 2 indicate measured cumulative offsets for the intermediate and deep gullies, respectively.

distribution and maximum intensity of reported damage suggest that these earthquakes produced surface ruptures. Paleoseismological studies show evidence of historical surface ruptures in trenches dug near Jericho and next to the Sea of Galilee, to the south and north of the fault segment, respectively (Reches and Hoexter, 1981; Marco et al., 2003).

5. Left-laterally offset drainage system

Major active faults very often display numerous geological and geomorphologic features that evidence the occurrence of recent tectonic movements likely associated with large earthquakes. From field observations and careful examination of aerial photos, we have identified 20 gullies along the southern section of the JVF that display systematic left-lateral offsets (Fig. 5). The detailed study including offset measurements at three sites (see Figs. 1 and 5) supports the relationship between the drainage pattern and surface faulting as identified on the aerial photographs. Aerial photographs were scanned at their resolution limit (600 dpi) and digitally enhanced (histogram stretching and contrast improvement). All measurements are considered to have a reading uncertainty of ±5 pixels which corresponds to ±5 m (given scale and resolution). Aside from two prominent rivers that are direct tributaries to the Jordan River, most gullies display a dendritic pattern and correspond to a complex regressive drainage network. The drainage system results from an intense erosion in combination with semi-arid climatic conditions and soft lacustrine sediments. Nowadays, the hydrographic system is multiple with intermittent (e.g., Wadi Russayf) and ephemeral (middle-sized and small gullies) streams. The dendritic pattern (with mostly east–west trending streams) shows incisions nearly orthogonal to and evenly distributed along the fault strike. The increasingly arid climate, as attested by the dramatic down-drop of the lake/sea level during the last 25 kyr (Fig. 2), favours the formation and preservation of incisions. In most cases, we have selected relatively long stream channels (>200 m) that are sufficiently distant to identify clear piercing points displacements. Beside the approach exemplified by McGill and Sieh (1991) to measure cumulative offsets from throughgoing streams, we develop a model specific to regressive erosion. From aerial photographs, field observations and depth analysis of gullies, we propose a mechanism that describes relationships between faulting and drainage development (Fig. 6). As the fault develops through soft lacustrine units, it forms a mechanically weak draining zone and creates favourable conditions for the localized inception of gullies. The latter may extend from the fault and orthogonally to it, and provide geomorphic markers of subsequent fault movements. Offset measurement does not only rely on a detailed depth analysis but also on the identification of inception points (Fig. 6) and the understanding of the history of gully formation.

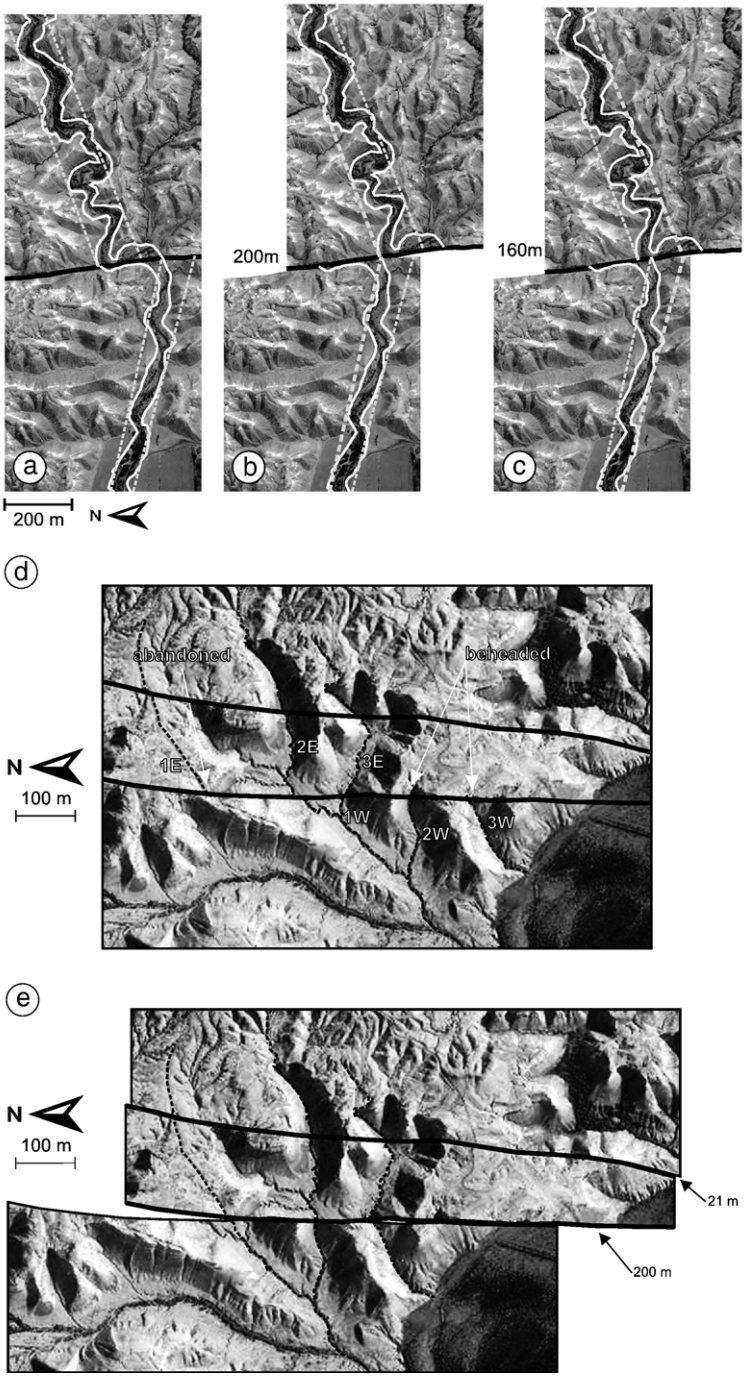

Fig. 7. Examples of reconstruction of long-term cumulative offsets affecting drainage at Ghor Katar and Ghor Al-Mendessa (see Fig. 1 for location). a) Present-day situation of Wadi Russayf. The eastern section of the stream exhibits clear meandering while the western is more linear, thus denoting different flow regimes across the fault. In order to determine the total offset, we delimited the meandering corridor of the stream on both sides of the fault (dashed grey lines). To match corresponding piercing points, one block needs to be retrodeformed by b) 200 m when considering the northern bank or c) 160 m when considering the southern bank. Hence, the mean offset affecting Wadi Russayf is estimated at 180 ± 20 m. d) Retrodeformation of a fork-shaped drainage at Ghor Al-Mendessa. Gully 1E is abandoned and gullies 2W and 3W are beheaded by the passage of the fault. Retrodeformation reveals a cumulative left-lateral offset of ~200 m across the main fault and ~21 m across a secondary fault. Since both branches affect the deepest generation of incisions, we assign a total displacement of 221 ± 25 m to that class at that site.

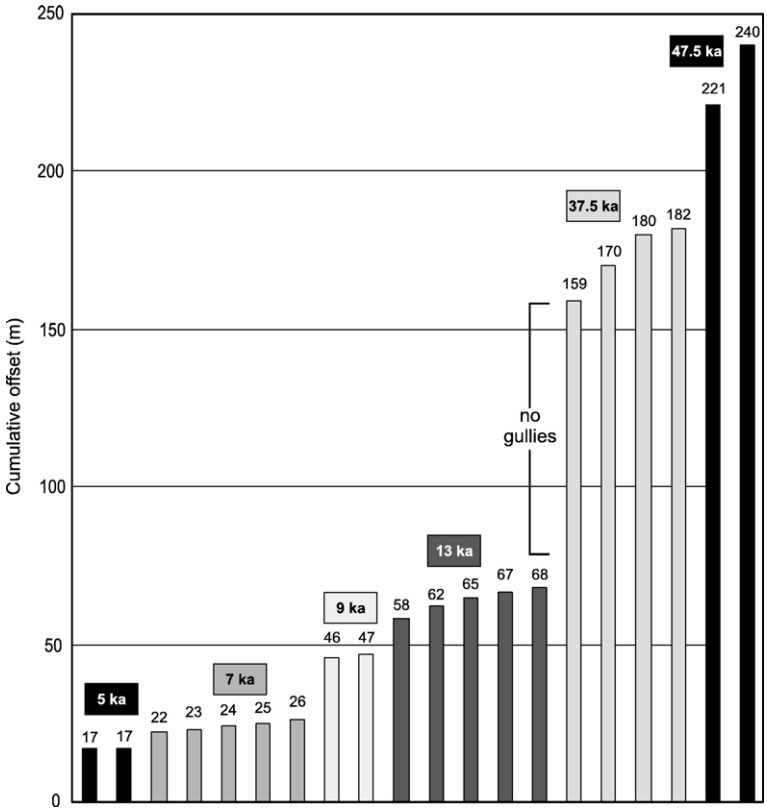

Fig. 8. Cumulative displacements obtained from offset gullies and streams. Values cluster into six distinct classes represented with different shades of grey. Increasing displacement values affect increasingly mature and deep gullies. Labels indicate the individual displacement values and boxed labels indicate the ages inferred from paleoclimatic correlations. One may note an obvious data gap between ~70 m and ~160 m due to the absence of corresponding incisions (see text for details).

Well-defined piercing points along the fault correspond to recent streams that show straight and narrow incisions, hence the overall uncertainty is given by the reading uncertainty (±5 m). In contrast, piercing points corresponding to meandering deep and wide streams, presumably older, and related offsets are difficult to measure and present an overall uncertainty of ±20 m. At K'tar El-Munkataates (Fig. 1b), the fault trace is linear and affects the drainage system showing twelve cumulative displacement values ranging from 17±5 m to 240±20 m (Fig. 5a). Several incisions were beheaded with their upstream section abandoned and a new one created by regressive erosion or captured by a previous stream. In Fig. 5a, left-lateral offsets are evidenced by the major channel showing 240±20 m, a few hundred meters further south two standalone streams show 24±5 m and 170± 20 m of left-lateral displacement. Further north, two beheaded streams show 182±20 m and 159±20 m of displacement and small stream channels clearly exhibit 65± 10 m and 26±5 m of left-lateral displacement. Finally, the northernmost channel shows 17±5 m of left-lateral offset.

At Ghor Katar (Fig. 1b), seven E–W to NE–SW trending river incisions are crossed by the fault and exhibit left-lateral offsets with values ranging from 17± 5 m to 180±20 m (Fig. 5b). In particular, Wadi Russayf is the most prominent E–W trending river channel and related incision cut by the JVF (Fig. 1b). The reconstruction of Fig. 7a–c indicates that the trend of the Wadi Russayf channel and related river banks can be matched without difficulty to yield a cumulative left-lateral displacement of 180±20 m. Furthermore, north of Wadi Russayf, an individual gully indicates 23±5 m of left-lateral offset. South of Wadi Russayf, prominent gully incisions show 58±10 m, 62±10 m and 22±5 m of left-lateral displacement (Fig. 5b). At Ghor Al-Mendessa (Fig. 1a), two sub-parallel fault branches display a left-stepping geometry (Fig. 5c). Among several geomorphic features along faults, clearly beheaded streams indicate left-lateral cumulative offsets (Fig. 7d). The reconstruction of Fig. 7e reveals fault displacements of 21±5 m for the easternmost branch and 200±20 m for the westernmost branch.

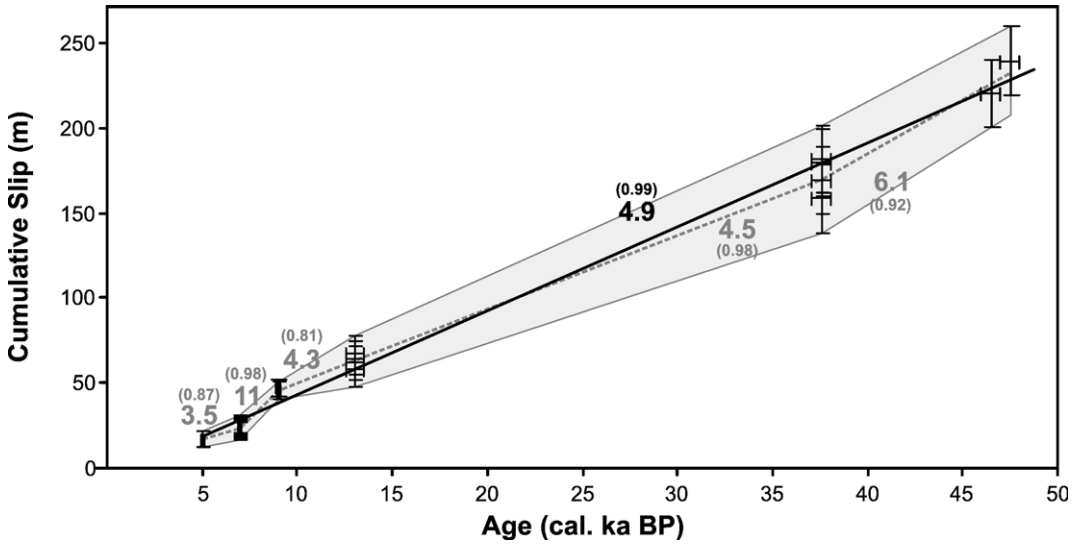

Fig. 9. Plot of cumulative slip affecting the different gully incisions versus their age inferred from climatic events. Considering a standard model involving a constant slip rate (black line and number), we calculate a mean value of 4.9±0.2 mm/yr for the last 47.5 kyr. With a variable slip rate model (grey dashed lines and numbers) values fluctuate between 3.5 mm/yr and 11 mm/yr over 2-kyr- to 24-kyr-long periods. Numbers between brackets are corresponding R^2 values.

The 20 cumulative displacements may be organized as a function of the depth of gullies and thus into six distinct classes (Fig. 8). Assuming that incision depth is proportional to age (Poesen et al., 2003) we may correlate the six classes of stream offsets to the age of incisions and hence to gully inception. Furthermore, the ages of gully inception can be correlated with the lake-level curve of Fig. 2 and the related six climatic events described in paragraph 3 (i.e., 5 ka, 7 ka, 9 ka, 13 ka, 37.5 ka and 47.5 ka). In this situation, the critical age determination of gully inception that relies on the high-resolution lake/sea level fluctuations (Fig. 2) may be considered as well defined, leaving little possibilities for alternative scenarios. Fig. 9 shows a plot of cumulative displacements affecting gullies as a function of their inferred age. The well-defined regression line (R^2=0.99) displays a slope of 4.9±0.2 mm/yr, thus providing a mean slip-rate for the JVF during the last 47.5 kyr.

6. Conclusions and discussion

6.1. Lake-level uncertainties and gully inception

Paleoclimatic fluctuations in the Dead Sea are constrained by a high-resolution stratigraphic succession, varve-counting, a large amount (>100) of isotopic dates, and detailed field investigations of paleoshorelines and geomorphology (Schramm et al., 2000; Bartov et al., 2002; Landmann et al., 2002; Bookman et al., 2004; Haase-Schramm et al., 2004). The spatial distribution of lacustrine deposits constitute another constraining factor for paleoclimatic studies. Hence, lake level and related climatic evolution as presented in Fig. 2 are well constrained.

The inceptions of gullies in the Jordan Valley are primarily related to the deposition of a thick section of lacustrine sediments and a subsequent down-drop of the water level. The dating of gully inception is constrained by the high-resolution lake-level and rainfall history as illustrated in Fig. 2. The Dead Sea region is a closed sea/lake without any output except evaporation and its watershed is entirely local. Therefore, any climatic change is recorded by lake-level fluctuations and geomorphology. An important factor is the homogeneous response to rainfall and rilling of the Lisan and Damya lacustrine deposits, which display no major lithological variations. In addition, the drainage systems at the three study sites were formed by regressive erosion and are isolated from the mountain front making them sensitive to very local processes such as rain-wash and lake-level fluctuations. Gullies may form during low lake-level periods and intense rainfall events, while periods of high lake-level rule out the generation of gullies. The age of gullies is hence intimately related to the down-drop of lake-level below the topographic surface at −295 m (at 47.5 ka, 37.5 ka and 13 ka) and major rainfall episodes (at 9 ka, 7 ka and 5 ka) as shown in Fig. 2. The high-resolution stratigraphy and related dating supported by varve-counting leave little possibility for a gap in the paleoclimatic

reconstruction. It is of interest to mention the variety of sources for lake-level variations based on geological evidence (Bartov et al., 2002; Bookman et al., 2004) and supported by archaeological and historical data (Enzel et al., 2003; Bookman et al., 2004).

The existence and related dating of the different generations of gullies and incisions constrain the maximum age of each class of cumulative displacements. Hence, the identification of six classes of displacements implies a chronological order for the inception and development of gullies. However, the absence of gullies within the record of cumulative slip between ~70 m and ~160 m illustrated in Fig. 8 spans ~24 kyr. Here, we note the remarkable coincidence between the absence of ~70–160 m cumulative slip and the high stand of lake-level between 14 ka and 36 ka, bearing in mind that gullies and incisions cannot be generated during high lake-level periods.

A peculiar observation is at Ghor Al-Mendessa where the local geomorphology is different from the northern sites and shows only two prominent classes of incisions (the deepest and the shallowest gullies). Here again, there is no possibility to record intermediate cumulative displacements at that site because the local surface topography is at −320 m, lower than the northern surface topography, and has continuously been under a minimum of 20 m of water between 43 ka BP and 13 ka BP.

6.2. Late Quaternary slip rate along the Dead Sea fault

The tectonic geomorphology along the JVF indicates evidence for late Pleistocene and Holocene surface ruptures. The Sea of Galilee and the Dead Sea correspond to tectonic structures that define the fault segment boundaries. However, the fault can be subdivided into sub-segments limited mainly by pressure ridges. The fault zone crosses the well-dated Lisan and Damya late Quaternary formations and left-laterally offsets a series of 20 gully incisions at K'tar El-Munkataates, Ghor Katar and Ghor Al-Mendessa with a maximum cumulative horizontal displacement of 240±20 m. Additionally, a maximum cumulative vertical displacement of 18.4±0.5 m is visible at Ghor Katar. Although the visible amount of vertical displacement can be sometimes erroneous in strike-slip faulting (because it strongly depends on the faulting/stratigraphy geometry), the constant horizontality of the "white cliff" and upper Lisan units (well visible in an extensive area of large incisions) and thickness variations across the fault attest to a syntectonic deposition against a growth fault. Combined with isotopic dating, as well as ages inferred from paleoclimatic fluctuations, these offset values yield slip rates of 4.9±0.2 mm/yr left-lateral and 0.2 mm/yr downdip for the last 47.5 kyr.

The 4.9±0.2 mm/yr slip rate is comparable to the 2 to 6 mm/yr obtained from an offset drainage system in the Wadi Araba (Klinger et al., 2000; Niemi et al., 2001) and offset stream channels at Beyt Zayda north of the Sea of Galilee (Marco et al., 2005). Recent GPS measurements between the Sinai block and the Arabia plate and a related tectonic model provide a 4.4±0.3 mm/yr slip rate along the JVF (Wdowinski et al., 2004; Reilinger et al., 2006). These estimated slip rates are, however, lower than the short term 6–7 mm/yr obtained from the paleoseismic study of a displaced Roman aqueduct and GPS measurements along the northern DSF in Syria (Meghraoui et al., 2003; McClusky et al., 2003). The 2–3 mm/yr difference between the southern and northern slip rates of the DSF can be explained with the location of the Euler pole of rotation offshore western Egypt as suggested by the GPS measurements (McClusky et al., 2003).

The long term 4.9±0.2 mm/yr slip rate along the JVF and the time elapsed since the 1033 AD large earthquake yield ~5 m of slip deficit along the JVF. This inference is valid, however, only if the ~1000 yr elapsed time corresponds to a periodic seismic cycle and previous earthquake clusters did not release most of the seismic energy of the fault rupture. The slip deficit is also consistent with the lack of earthquakes over the past few centuries along other fault segments in Syria and Lebanon. This points to the imminent occurrence of large earthquakes along the DSF. Considering a mean coseismic displacement of 3.5–5 m, a rupture length of 110 km and a seismogenic crust thickness of at least 20 km (Aldersons et al., 2003), the incipient event may produce a Mw ~7.4 earthquake (Kanamori and Anderson, 1975). The level of seismic hazard and risk along the Jordan Valley should be urgently re-evaluated taking into account the slip deficit.

As shown in the diagram of Fig. 9, possible variations of the slip rate through time along the JVF indicate values ranging from 3.5 mm/yr to 11 mm/yr. A comparable factor of three increase in slip rate has also been described by Weldon et al. (2004) from extensive paleoseismic studies along the southern San Andreas fault, where slip rate increases from 3.1 cm/yr to 8.9 cm/yr during a 300 yrs period. The high-resolution of the stratigraphic analysis and related isotopic dating provides a good constraint on the timing of cumulative displacements. Hence, the history of fault slip rates obtained from the analysis of paleoclimatic fluctuations indicates significant variations during the last ~50 kyr. This slip rate variation suggests an episodic faulting behaviour apparently in agreement with the historical

seismicity catalogue and related earthquake distribution in 64 BC, 31 BC, AD 749 and AD 1033 and the related seismic gap until the present day (Abou Karaki, 1987; Ambraseys and Jackson, 1998; Sbeinati et al., 2005).

Acknowledgments

Authors are indebted to the Deanship of scientific research (University of Jordan), the Jordan Valley Authority, the Natural Resources Authority and the Military Commandment for their assistance and help during our field investigations. We thank Prof. A. Abed (Univ. of Jordan) for fruitful discussions on the Lisan and Damya formations. We also thank Daniel Mège and Chris Okubo for their very detailed and constructive reviews. This study is funded by the EC 5th Framework Program and APAME project (Contract ICA3-CT-2002-10024). SPOT 5 satellite images were provided by the ISIS program (file ISIS0503-759).

References

Abed, A.M., Yaghan, R., 2000. On the paleoclimate of Jordan during the last glacial maximum. Palaeogeogr. Palaeoclimatol. Palaeoecol. 160, 23–33.

Abou Karaki, N., 1987. Synthèse et carte sismotectonique des pays de la bordure orientale de la Méditerrannée: Sismicité du système de failles du Jourdain- Mer Morte, PhD, Université Louis Pasteur.

Aldersons, F., Ben Avraham, Z., Hofstetter, A., Kissling, E., Al Yazjeen, T., 2003. Lower-crustal strength under the Dead Sea basin from local earthquake data and rheological modeling. Earth Planet. Sci. Lett. 214, 129–142.

Al-Taj, M., 2000. Active Faulting Along the Jordan Valley Segment of the Jordan–Dead Sea Transform. University of Jordan.

Ambraseys, N.N., Jackson, J.A., 1998. Faulting associated with historical and Recent earthquakes in the eastern Mediterranean region. Geophys. J. Int. 133, 390–406.

Bartov, Y., Stein, M., Enzel, Y., Agnon, A., Reches, Z.E., 2002. Lake Levels and Sequence Stratigraphy of Lake Lisan, the Late Pleistocene Precursor of the Dead Sea. Quat. Res. 57, 9–21.

Bookman, R., Enzel, Y., Agnon, A., Stein, M., 2004. Late Holocene lake levels of the Dead Sea. Geol. Soc. Amer. Bull. 116, 555–571.

Bloom, A.L., 1991. Geomorphology: a Systematic Analysis of Late Cenozoic Landforms. Prentice-Hall. 532 pp.

El-Isa, Z.H., Mustafa, H., 1986. Earthquake deformations in the Lisan deposits and seismotectonic implications. Geophys. J. R. Astron. Soc. 86, 413–424.

Enzel, Y., Bookman, R., Sharon, D., Gvirtzman, H., Dayan, U., Ziv, B., Stein, M., 2003. Late Holocene climates of the Near East deduced from Dead Sea level variations and modern regional winter rainfall. Quat. Res. 60, 263–273.

Enzel, Y., Agnon, A., Stein, M., 2006. New Frontiers in Dead Sea Paleoenvironmental Research. Geological Society of America, Boulder.

Galli, P., 1999. Active tectonics along the Wadi Araba-Jordan Valley transform fault. J. Geophys. Res., B, [Solid Earth Planets] 104, 2777–2796.

Garfunkel, Z., Zak, I., Freund, R., 1981. Active faulting in the Dead Sea Rift. The Dead Sea Rift; selected papers of the International symposium on the Dead Sea Rift 80. Special Issue, vol. 1–4. Elsevier, Amsterdam, Netherlands, pp. 1–26.

Guidoboni, E., Comastri, A., Traina, G., 1994. Catalogue of Ancient Earthquakes in the Mediterranean Area up to the 10th Century. ING-SGA, Bologna. 504 pp.

Haase-Schramm, A., Goldstein, S.L., Stein, M., 2004. U–Th dating of Lake Lisan (late Pleistocene Dead Sea) aragonite and implications for glacial East Mediterranean climate change. Geochim. Cosmochim. Acta 68, 985–1005.

Kanamori, H., Anderson, D.G., 1975. Theoretical basis of some empirical relations in seismology. Bull. Seismol. Soc. Am. 65, 1073–1095.

Klinger, Y., Avouac, J.-P., Abou Karaki, N., Dorbath, L., Bourles, D., Reyss, J.L., 2000. Slip rate on the Dead Sea transform in northern Araba Valley (Jordan). Geophys. J. Int. 142, 755–768.

Landmann, G., Abu Qudaira, G.M., Shawabkeh, K., Wrede, V., Kempe, S., 2002. Geochemistry of the Lisan and Damya Formations in Jordan, and implications for paleoclimate. Quat. Int. 89, 45–57.

Malkawi, A.I.H., Alawneh, A.S., 2000. Paleoearthquake Features as Indicators of Potential Earthquake Activities in the Karameh Dam Site. Nat. Hazards 22, 1–16.

Marco, S., Stein, M., Agnon, A., Ron, H., 1996. Long-term earthquake clustering: A 50,000-year paleoseismic record in the Dead Sea Graben. J. Geophys. Res. 101, 6179–6192.

Marco, S., Hartal, M., Hazan, N., Lev, L., Stein, M., 2003. Archaeology, history, and geology of the A.D. 749 earthquake, Dead Sea Transform. Geology (Boulder) 31, 665–668.

Marco, S., Rockwell, T.K., Heimann, A., Frieslander, U., Agnon, A., 2005. Late Holocene activity of the Dead Sea Transform revealed in 3D paleoseismic trenches on the Jordan Gorge segment. Earth Planet. Sci. Lett. 234, 189–205.

McClusky, S., Reilinger, R., Mahmoud, S., Ben, S.D., Tealeb, A., 2003. GPS constraints on Africa (Nubia) and Arabia plate motions. Geophys. J. Int. 155, 126–138.

McGill, S.F., Sieh, K., 1991. Surficial offsets on the central and eastern Garlock Fault associated with prehistoric earthquakes. J. Geophys. Res., B, [Solid Earth Planets] 96, 21,597–521,621.

Meghraoui, M., Gomez, F., Sbeinati, R., Van der Woerd, J., Mouty, M., Darkal, A., Radwan, Y., Layyous, I., Najjar, H.M., Darawcheh, R., Hijazi, F., Al-Ghazzi, R., Barazangi, M., 2003. Evidence for 830 years of seismic quiescence from paleoseismology, archeoseismology and historical seismicity along the Dead Sea fault in Syria. Earth Planet. Sci. Lett. 210, 35–52.

Niemi, T.M., Zhang, H., Atallah, M., Harrison, J.B.J., 2001. Late Pleistocene and Holocene slip rate of the Northern Wadi Araba fault, Dead Sea Transform, Jordan. J. Seismol. 5, 449–474.

Poesen, J., Nachtergaele, J., Verstraeten, G., Valentin, C., 2003. Gully erosion and environmental change; importance and research needs. Catena 50 (2–4), 91–133.

Poirier, J.-P., Taher, M.A., 1980. Historical seismicity in the near and Middle East, North Africa, and Spain from Arabic documents (VIIth–XVIIIth century). Bull. Seismol. Soc. Am. 70, 2185–2201.

Reches, Z.E., Hoexter, D.F., 1981. Holocene seismic and tectonic activity in the Dead Sea area. The Dead Sea Rift; selected papers of the International symposium on the Dead Sea Rift 80. Special Issue, vol. 1–4. Elsevier, Amsterdam, Netherlands, pp. 235–254.

Reilinger, R., McClusky, S., Vernant, P., Lawrence, S., 2006. GPS constraints on continental deformation in the Africa–Arabia–Eurasia continental collision zone and implications for the dynamics of plate interactions. J. Geophys. Res. 111. doi:10.1029/2005JB004051.

Savage, S.H., Zamora, K., Keller, D.R., 2003. Archaeology in Jordan, 2002 Season. Am. J. Archaeol. 107, 449–475.

Sbeinati, M.R., Darawcheh, R., Mouty, M., 2005. The historical earthquakes of Syria; an analysis of large and moderate earthquakes from 1365 B.C. to 1900 A.D. Ann. Geophys. 48, 347–435.

Schramm, A., Stein, M., Goldstein, S.L., 2000. Calibration of the 14C time scale to >40 ka by 234U – 230Th dating of Lake Lisan sediments (last glacial Dead Sea). Earth Planet. Sci. Lett. 175, 27–40.

Wdowinski, S., Bock, Y., Baer, G., Prawirodirdjo, L., Bechor, N., Naaman, S., Knafo, R., Forrai, Y., Melzer, Y., 2004. GPS measurements of current crustal movements along the Dead Sea fault. J. Geophys. Res. 109, B05403.

Weldon, R., Scharer, K., Fumal, T., Biasi, G., 2004. Wrightwood and the earthquake cycle: What a long recurrence record tells us about how faults work. GSA Today 14, 4–10.

Wells, D.L., Coppersmith, K.J., 1994. New empirical relationships among magnitude, rupture length, rupture width, rupture area, and surface displacement. Bull. Seismol. Soc. Am. 84, 974–1002.

Wesnousky, S.G., 2006. Predicting the endpoints of earthquake ruptures. Nature 444, 358–360.